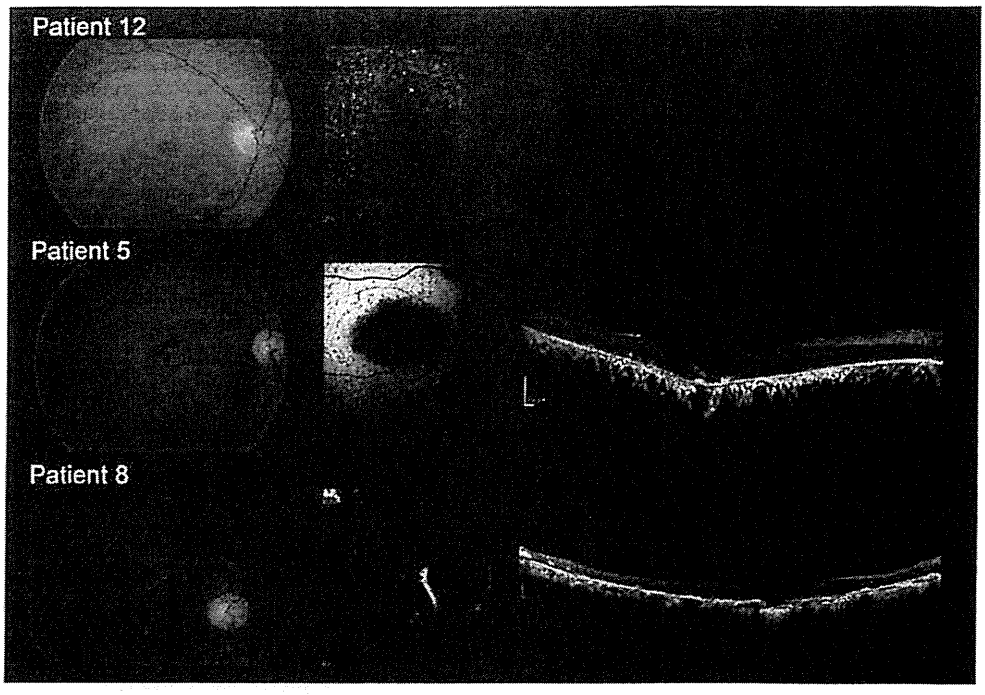

Figure 2. Color fundus photographs (left), autofluorescence (AF) images (middle), and optical coherence tomography (OCT) images (right) of 3 representative cases with Stargardt's disease harboring homozygous missense alleles, showing a mild phenotype in patient 12, a moderated phenotype in patient 5, and a severe phenotype in patient 8.

14 patients (Table 3). One patient (7%) had a type 1 AF pattern, 12 patients (86%) had a type 2 pattern, and 1 patient (7%) had a type 3 pattern. Optical coherence tomography images were available in 8 patients (Table 3). Central foveal thickness ranged from 31 to 128 μm. Six patients (75%; patients 1, 2, 3, 5, 11, and 13) showed foveal atrophy in both the neurosensory retina and the RPE, with disruption observed mainly in outer retinal layers at the macula; 2 patients (25%; patients 8 and 9) had a disrupted outer retinal layer with preserved inner retinal layers at the macula. Electrophysiologic assessment was available in 18 patients (Table 3). Five patients (28%) had a group 1 ERG, and 13 patients (72%) had a group 3 ERG.

Molecular Genetics

Mutational screening was performed with the APEX technology in 12 probands (patients 1, 3, 5, 6, 8, 9, 11, 12, 13, 14, 15, and 18), and the high-throughput NGS was applied to 1 proband (patient 3). Ten homozygous *ABCA4* variants that likely cause disease were detected in 18 patients. Detailed results including in silico analysis to predict pathogenicity are shown in Table 4 (available at http://aaojournal.org).

Eleven patients (61%) had homozygous missense variants, and 7 (39%) were homozygous for presumed null variants (Table 3). Of 13 variants identified, 9 were missense variants and 4 were presumed null variants. The 4 null variants include 1 frame shift (p.Glu905fsX916), 2 stops (p.Arg1300X and p.Gln2220X), and 1 intronic variant (c.4253+4C>T), which is likely to disrupt the splice-donor site of intron 28. Coexistence of 2 homozygous missense variants was observed in 2 patients (patients 3 and 5). One putative novel variant (p.Glu905fsX916) was identified by NGS, and 7 have not been described in the homozygous state before: p.Val931Met, p.Cys1488Arg, p.Arg1705Gln, p.Leu2027-Phe, p.Arg1300X, c.4253+4C>T, and p.Gln2220X (Table 4, available at http://aaojournal.org). A schematic of the *ABCA4* protein structure showing the position of the missense variants detected in this study is presented in Figure 5 (available at http://aaojournal.org).

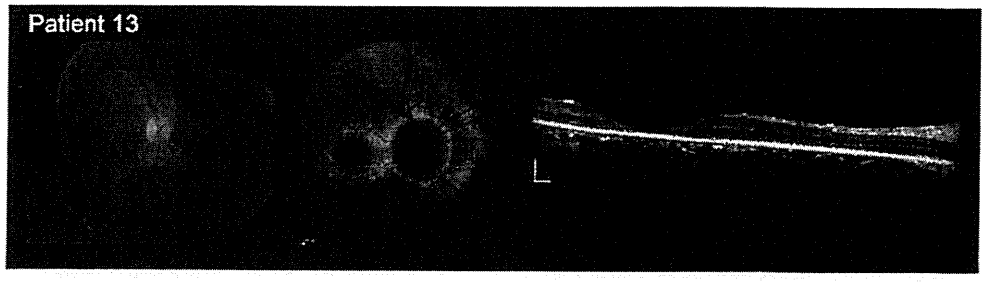

Figure 3. Color fundus photographs (left), autofluorescence (AF) images (middle), and optical coherence tomography (OCT) images (right) of 1 representative case with a severe phenotype of Stargardt's disease harboring homozygous null alleles (patient 13).

Sorting Intolerant from Tolerance (available at: http://sift.jcvi.org/; accessed November 1, 2012)[37] and PolyPhen2 (available at: http://genetics.bwh.harvard.edu/pph/index.html; accessed November 1, 2012).[38] A frequency for each allele was estimated with reference to the Exome Variant Server (National Heart, Lung, and Blood Institute Exome Sequencing Project, Seattle, WA; available at: http://snp.gs.washington.edu/EVS/; accessed November 1, 2012).

Previously reported variants that likely do not cause disease (polymorphisms) also were screened by the APEX technology in probands of each family to define the chromosomal haplotype for the alleles detected in this study.[2,12,21]

Results

Clinical Findings

Eighteen patients from 13 families were included in the study. The clinical, genetic, and electrophysiologic findings are summarized in Table 3. There were 12 male and 6 female patients. Fourteen patients from 9 families are originally from South Asia, 2 patients from 2 families are from Middle East Asia, and 2 patients from 2 families are from Europe. There were 3 sibling pairs (patients 1 and 2, 6 and 7, and 9 and 10) and a further family with 2 affected siblings and an affected cousin (patient 16, 17, and 18 respectively; Fig 1, available at http://aaojournal.org). Consanguinity was reported in 11 families: 7 first cousin marriages, 1 uncle-niece marriage, 1 second cousin once removed marriage, and 2 unknown related marriages (Table 3). One patient had delayed developmental milestones as an infant (patient 3).

All affected patients except for 1 (patient 12) had central visual loss, with the age of onset ranging from 3 to 30 years (Table 3). One individual with few symptoms was referred because of fundus abnormality at the age of 40 years (patient 12). Seven patients had early onset (<10 years) (patients 3, 4, 13, 14, 15, 16, and 17). The age at examination ranged from 7 to 48 years, and the duration of disease ranged from 0 to 39 years. The logMAR visual acuities ranged from 0.0 to 3.0, and 3 patients (17%; patients 10, 11, and 12) had a logMAR visual acuity better than 1.0 in at least 1 eye. One patient (patient 12) had preserved logMAR visual acuity, with 0.18 in the right eye and 0.0 in the left eye.

Color fundus photographs, AF images, and OCT images of representative cases with each variant are shown in Figures 2 and 3: 3 representative cases with missense variants in Figure 2 and 1 case with presumed null variants in Figure 3. Electrophysiologic traces of 4 representative cases are shown in Figure 4.

Of 18 patients, 5 (28%) had a type 1 fundus appearance, 9 (50%) had a type 2 appearance, and 4 (22%) had a type 3 appearance (Table 3). Autofluorescence images were available in

Table 3. Summary of Clinical and Molecular Status of 18 Patients with ABCA4 Homozygous Variants

Pt No.	FM No.	Sex	Ethnicity	Consanguinity	Age at Onset (yrs)	Age (yrs)	Duration of Disease (yrs)	LogMAR VA RE	LogMAR VA LE	Fundus Appearance	AF Pattern	ERG Group	OCT Central Foveal Thickness (μm) RE	OCT Central Foveal Thickness (μm) LE	Mutation Status
1	1	M	S Asian	Yes (1st cousin)	11	33	22	1.0	1.0	2	2	1	64	69	c.634 C>T, p.Arg212Cys
2	1	F	S Asian	Yes (1st cousin)	11	36	25	1.0	1.0	2	2	3	31	41	c.634 C>T, p.Arg212Cys
3*	2	M	European	No	3	8	5	1.2	1.2	2	2	3†	41	36	c.1622 T>C, p.Leu541Pro / c.3113 C>T, p.Ala1038Val
4	3	F	S Asian	Yes (2nd cousin once removed)	5	8	3	1.0	1.0	2	2	3	NA	NA	c.2713delG, p.Glu905fsX916
5	4	M	S Asian	Yes (unknown)	10	25	15	1.0	1.08	2	2	3	64	60	c.2791 G>A, p.Val931Met / c.5114 G>A, p.Arg1705Gln
6	5	M	S Asian	Yes (1st cousin)	10	30	20	1.0	1.0	2	2	3	NA	NA	c.4462 T>C, p.Cys1488Arg
7	5	F	S Asian	Yes (1st cousin)	10	22	12	2.0	1.0	2	2	3	NA	NA	c.4462 T>C, p.Cys1488Arg
8	6	M	ME Asian	Yes (1st cousin)	30	36	6	1.08	2.0	3	3	3	103	95	c.4918 C>T, p.Arg1640Trp
9	7	F	S Asian	Yes (2nd cousin)	19	27	8	1.78	2.0	1	2	1	128	90	c.5882 G>A, p.Gly1961Glu
10	7	M	S Asian	Yes (2nd cousin)	30	34	4	0.48	0.48	1	2	1	NA	NA	c.5882 G>A, p.Gly1961Glu
11	8	F	S Asian	Yes (1st cousin)	17	26	9	0.78	0.78	1	1	1	54	47	c.5882 G>A, p.Gly1961Glu
12	9	F	European	No	44	44	0	0.18	0.0	2	2	1	NA	NA	c.6079 C>T, p.Leu2027Phe
13	10	M	ME Asian	Yes (1st cousin)	5	11	6	1.3	1.0	3	2	3	62	68	c.3898 C>T, p.Arg1300X
14	11	M	S Asian	Yes (unknown)	8	11	3	1.0	1.0	2	2	3	NA	NA	c.4253+4 C>T
15	12	M	S Asian	Yes (1st cousin)	9	48	39	3.0	3.0	3	NA	3	NA	NA	c.6658 C>T, p.Gln2220X
16	13	M	S Asian	Yes (uncle and niece)	4	7	3	1.08	1.08	1	NA	3	NA	NA	c.6658 C>T, p.Gln2220X
17	13	M	S Asian	Yes (uncle and niece)	6	8	2	1.08	1.0	1	NA	3	NA	NA	c.6658 C>T, p.Gln2220X
18	13	M	S Asian	Yes (1st cousin)	17	25	8	1.78	1.78	3	NA	3	NA	NA	c.6658 C>T, p.Gln2220X

AF = autofluorescence; ERG = electroretinography; F = female; FM No. = family number; LE = left eye; LogMAR VA = logarithm of the minimum angle of resolution; M = male; ME Asian = middle east Asian; NA = not applicable; OCT = optical coherence tomography; Pt = patient; RE = right eye; S Asian = south Asian.

The age of onset was defined as either the age at which visual loss was first noted by the patient, or as the age at the latest examination for patients who were asymptomatic. The duration of the disease was calculated as the difference between age at onset and age at the latest examination. The central foveal thickness was defined as the distance between inner retinal surface and inner border of retinal pigment epithelium.

*Patient 3 had delayed developmental milestones as an infant.

†The single flash cone ERG and scotopic bright flash ERG were electronegative in patient 3.

alleles by means of clinical features, retinal imaging, and electrophysiologic examination.

Methods

Patients

Patients with homozygous *ABCA4* alleles were identified from a cohort of 276 patients with a clinical diagnosis of *ABCA4*-related retinal disease presenting to the retinal genetics clinics at Moorfields Eye Hospital. After informed consent was obtained, blood samples were taken from all individuals for DNA extraction and mutation screening of *ABCA4*. The protocol of the study adhered to the provisions of the Declaration of Helsinki and was approved by the Ethics Committee of Moorfields Eye Hospital.

Clinical Assessment

A detailed medical history was obtained, and a comprehensive ophthalmological examination was performed. The age of onset was defined as the age at which visual loss was first noted by the patient or the age at the latest examination for patients who were asymptomatic. The duration of the disease was calculated as the difference between age at onset and age at the latest examination. Clinical assessment included best-corrected Snellen visual acuity (converted to equivalent logarithm of the minimum angle of resolution [logMAR]), ophthalmoscopy, fundus photography, autofluorescence (AF) imaging, spectral-domain optical coherence tomography (SD-OCT), and electrophysiologic assessment.

Color fundus photography was performed with the TRC-50IA Retinal Fundus Camera (Topcon, Inc., Tokyo, Japan), and patients were divided into 1 of 3 types, in keeping with a previous classification of ophthalmoscopic findings[8]: (1) patients with an atrophic-appearing foveal lesion(s) with or without perifoveal yellowish-white deposits; (2) subjects with an atrophic-appearing foveal/macular lesion and numerous yellowish-white deposits throughout the posterior pole, extending anteriorly to the vascular arcades and nasally to the optic disc; and (3) individuals with extensive atrophic-appearing changes of the retinal pigment epithelium (RPE) throughout the posterior pole, extending beyond the vascular arcades (Table 1, available at http://aaojournal.org).

Autofluorescence imaging was performed using Spectralis with viewing module version 5.1.2.0 (Heidelberg Engineering, Heidelberg, Germany; excitation wavelength, 488 nm; barrier filter, 500 nm; field of view, 30×30° and 55×55°) after pupillary dilation. Patients were classified into 1 of 3 patterns, which was partially modified according to a previous report based on the AF findings[29]: (1) patients with a localized low AF signal at the fovea surrounded by a homogeneous background with or without perifoveal foci of high or low signal; (2) subjects with a localized low AF signal at the macula surrounded by a heterogeneous background and widespread foci of a high or low AF signal extending anterior to the vascular arcades; and (3) individuals with multiple areas of low AF signal at the posterior pole with a heterogeneous background with or without foci of a high or low AF signal (Table 1, available at http://aaojournal.org).

Spectral-domain OCT imaging was obtained with Spectralis with viewing module version 5.1.2.0. Central foveal thickness was defined as the distance between the inner retinal surface and the inner border of the RPE.[30,31] HEYEX software interface (version 1.6.2.0; Heidelberg Engineering) was used for obtaining a thickness measurement.[31]

Electrophysiologic assessment included full-field electroretinography (ERG) and pattern electroretinography (PERG) incorporating the standards of the International Society for Clinical Electrophysiology of Vision.[32,33] Electroretinography examination included (1) dark-adapted (DA) dim flash 0.01 $cd \cdot s \cdot m^{-2}$ (DA 0.01), (2) dark-adapted bright flash 11.0 $cd \cdot s \cdot m^{-2}$ (DA 11.0), (3) light-adapted (LA) 3.0 $cd \cdot s \cdot m^{-2}$ 30 Hz flicker ERG (LA 30 Hz), and (4) light-adapted 3.0 $cd \cdot s \cdot m^{-2}$ at 2 Hz (LA 3.0). Pattern ERG P50 was used to measure macular function; in this study, PERG reduction was considered severe if the P50 component was 0.6 μV or less (lower limit of normal, 2.0 μV). The electrophysiologic phenotype was based on a previous classification[34]: (1) patients with PERG P50 abnormality with normal ERGs, (2) subjects with PERG P50 abnormality and additional generalized cone ERG abnormality (assessed with LA 30 Hz and LA 3.0), and (3) individuals with PERG P50 abnormality and additional generalized cone and rod ERG abnormality (the latter assessed using DA 0.01 and DA 11.0) (Table 1, available at http://aaojournal.org).

The classification of severity for the phenotype of *ABCA4*-related retinal disease was performed on the basis of the clinical findings: age of onset, logMAR visual acuity, fundus appearance, AF pattern, and electrophysiologic grouping (Table 2).

Mutation Screening

Mutation analysis was performed with the solid-phase arrayed primer extension (APEX) technology (ABCR400 chip, Asper Ophthalmics, Tartu, Estonia) in 12 probands[35] and with high-throughput next-generation DNA sequencing (NGS) in 1 proband.[36] Direct Sanger sequencing was performed in siblings, parents, and other relatives of the probands when available to confirm segregation of alleles.

Null variants were defined as those expected to affect pre-mRNA splicing of the transcript or introduce a premature truncating codon. The term *variants* for purposes of this study includes those sequence changes previously shown to be enriched in patients with Stargardt's disease from prior studies. Missense variants were analyzed using 2 software prediction programs:

Table 2. Classification of Severity for the Phenotype of *ABCA4*-Related Retinal Disease

	Onset of Disease (yrs)	LogMAR VA in the Better Eye	Fundus Appearance	AF Type	ERG Group
Mild phenotype	Later onset (>15)	<0.78	1	1	1
Moderate phenotype	Patients who did not meet at least 2 criteria of either mild phenotype or severe phenotype were classified into the moderate phenotype subgroup.				
Severe phenotype	Early onset (<10)	>1.0	3	3	3

AF = autofluorescence; ERG = electroretinography; LogMAR VA = log minimum angle of resolution visual acuity.
For the purpose of this study, patients who met at least 2 criteria of mild phenotype were classified into the mild phenotype subgroup and those who had at least 2 features of severe phenotype were classified into the severe phenotype subgroup.

The Clinical Effect of Homozygous *ABCA4* Alleles in 18 Patients

Kaoru Fujinami, MD,[1,2,3,4] *Panagiotis I. Sergouniotis, MD,*[1,2] *Alice E. Davidson, PhD,*[1,2] *Donna S. Mackay, PhD,*[1,2] *Kazushige Tsunoda, MD,*[3] *Kazuo Tsubota, MD,*[4] *Anthony G. Robson, PhD,*[1,2] *Graham E. Holder, MD,*[1,2] *Anthony T. Moore, MD,*[1,2] *Michel Michaelides, MD,*[1,2] *Andrew R. Webster, MD*[1,2]

Purpose: To describe the phenotypic presentation of a cohort of individuals with homozygous disease-associated *ABCA4* variants.

Design: Retrospective case series.

Participants: Eighteen affected individuals from 13 families ascertained from a total cohort of 214 families with *ABCA4*-related retinal disease presenting to a single center.

Methods: A detailed history was obtained, and color fundus photography, autofluorescence (AF) imaging, optical coherence tomography (OCT), and electrophysiologic assessment were performed. Phenotypes based on ophthalmoscopy, AF, and electrophysiology were assigned using previously reported characteristics. *ABCA4* mutation detection was performed using the ABCR400 microarray (Asper Biotech, Tartu, Estonia) and high-throughput DNA sequencing, with direct sequencing used to assess segregation.

Main Outcome Measures: Detailed clinical, electrophysiologic, and molecular genetic findings.

Results: Eleven disease-associated homozygous *ABCA4* alleles were identified, including 1 frame shift, 2 stops, 1 intronic variant causing splice-site alteration, 2 complex missense variants, and 5 missense variants: p.Glu905fsX916, p.Arg1300X, p.Gln2220X, c.4253+4 C>T, p.Leu541Pro and p.Ala1038Val (homozygosity for complex allele), p.Val931Met and p.Arg1705Gln (complex allele), p.Arg212Cys, p.Cys1488Arg, p.Arg1640Trp, p.Gly1961Glu, and p.Leu2027Phe. Eight of these 11 homozygous alleles have not been reported previously. Six of 7 patients with homozygous null alleles had early-onset (<10 years) disease, with all 7 having a severe phenotype. Two patients with homozygous missense variants (p.Leu541Pro and p.Ala1038Val [complex], and p.Arg1640Trp) presented with a severe phenotype. Three patients with homozygous p.Gly1961Glu had adult-onset disease and a mild phenotype. One patient with homozygous p.Leu2027Phe showed a spared fovea and preserved visual acuity.

Conclusions: The phenotypes represented in patients identified as homozygous for presumed disease-associated *ABCA4* variants gives insight into the effect of individual alleles. Null alleles have severe functional effects, and certain missense variants are similar to nulls, suggesting complete abrogation of protein function. The common alleles identified, p.Gly1961Glu and p. Leu2027Phe, both have a mild structural and functional effect on the adult retina; the latter is associated with relatively retained photoreceptor architecture and function at the fovea.

Financial Disclosure(s): The author(s) have no proprietary or commercial interest in any materials discussed in this article. *Ophthalmology 2013;120:2324-2331 © 2013 by the American Academy of Ophthalmology.*

Stargardt's disease is the most common form of inherited macular dystrophy and is caused by recessive mutations in the gene *ABCA4* (Online Mendelian Inheritance in Man 601691; cytogenetic location, 1p 22.1; genomic coordinates [GRCh37], 1:94,458,392–94,586,704).[1–3] More than 600 variants have been reported to date.[4–22] Marked genetic heterogeneity confounds attempts to establish genotype–phenotype correlations. The lack of a readily exploitable functional assay of adenosine triphosphatase activity also limits the ability to investigate the functional consequences of individual *ABCA4* variants.[13]

Nevertheless, many reports have attempted to investigate the relationship between genotype and phenotype.[7,9,12,14,16,19,20,23,24] Determining the severity of specific alleles is confounded by the high prevalence of individuals who have compound heterozygous variants in *ABCA4*.[2,13] In only a few studies is it possible to evaluate the effects of specific variants.[12,14,20,22,23,25] Individuals who have homozygous variants in *ABCA4* offer a valuable opportunity to investigate the phenotype associated with specific single variants. There are a number of reports of families or small case series describing the phenotypic features of homozygous patients,[6,10,11,22,25–28] and 1 report features homozygous patients with 1 specific common allele (p.Gly1961Glu).[12] However, studies of large cohorts are still lacking because of the rarity of such homozygous cases.

We examined a cohort of homozygous patients to gain insights into the retinopathy caused by specific *ABCA4*

ISSN 0161-6420/13/$ - see front matter
http://dx.doi.org/10.1016/j.ophtha.2013.04.016

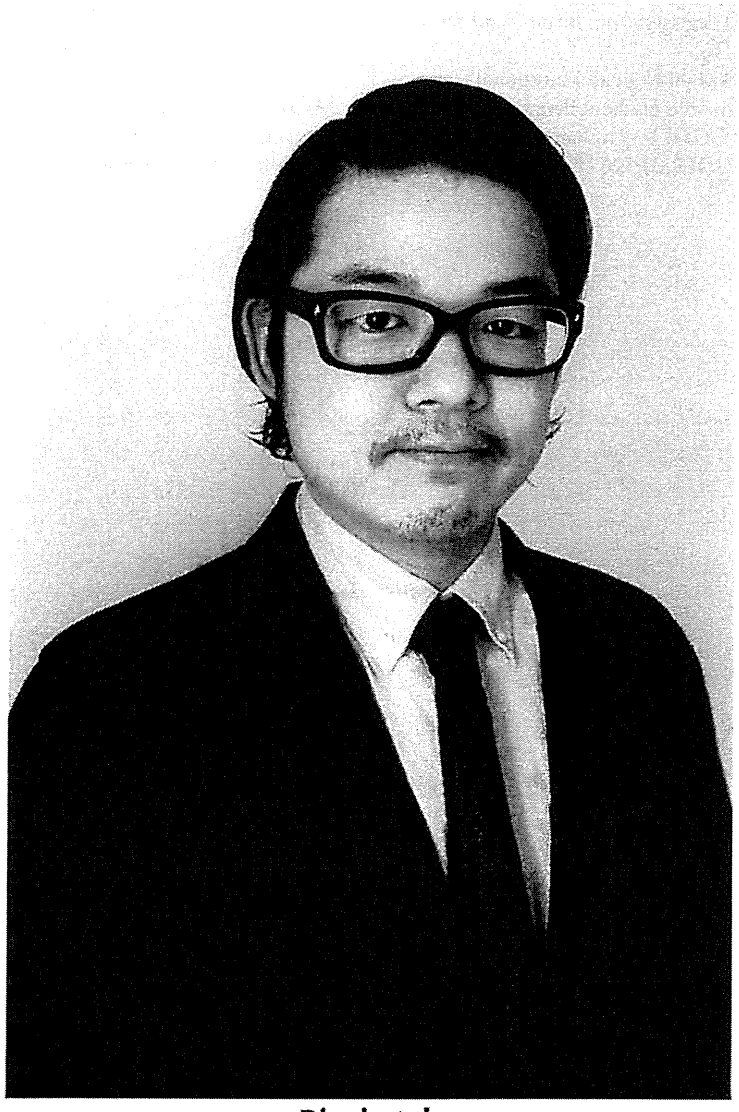

Biosketch

Kaoru Fujinami, MD is a clinical ophthalmologist and principal investigator at the National Institute of Sensory Organs associated with Keio University, School of Medicine, Tokyo, Japan. He has completed fellowships at Moorfields Eye Hospital and University College London, Institute of Ophthalmology, London, United Kingdom. His research interests include retinal disease, clinical electrophysiology, inherited eye disease and molecular genetics. His current projects relate to genotype-phenotype correlations in inherited retinal disease.

degeneration or cone-rod degeneration. *Invest Ophthalmol Vis Sci* 2001;42(10):2229–2236.
52. Fumagalli A, Ferrari M, Soriani N, et al. Mutational scanning of the ABCR gene with double-gradient denaturing-gradient gel electrophoresis (DG-DGGE) in Italian Stargardt disease patients. *Hum Genet* 2001;109(3):326–338.
53. Webster AR, Heon E, Lotery AJ, et al. An analysis of allelic variation in the ABCA4 gene. *Invest Ophthalmol Vis Sci* 2001; 42(6):1179–1189.
54. Rosenberg T, Klie F, Garred P, Schwartz M. N965S is a common ABCA4 variant in Stargardt-related retinopathies in the Danish population. *Mol Vis* 2007;13:1962–1969.

19. Burke TR, Rhee DW, Smith RT, et al. Quantification of peripapillary sparing and macular involvement in Stargardt Disease (STGD1). *Invest Ophthalmol Vis Sci* 2011;52(11): 8006–8015.
20. Klevering BJ, Blankenagel A, Maugeri A, Cremers FP, Hoyng CB, Rohrschneider K. Phenotypic spectrum of autosomal recessive cone-rod dystrophies caused by mutations in the ABCA4 (ABCR) gene. *Invest Ophthalmol Vis Sci* 2002;43(6):1980–1985.
21. Michaelides M, Chen LL, Brantley MA Jr, et al. ABCA4 mutations and discordant ABCA4 alleles in patients and siblings with bull's-eye maculopathy. *Br J Ophthalmol* 2007; 91(12):1650–1655.
22. Burke TR, Tsang SH, Zernant J, Smith RT, Allikmets R. Familial discordance in Stargardt disease. *Mol Vis* 2012;18: 227–233.
23. Burke TR, Fishman GA, Zernant J, et al. Retinal phenotypes in patients homozygous for the G1961E mutation in the ABCA4 gene. *Invest Ophthalmol Vis Sci* 2012;53(8): 4458–4467.
24. Cella W, Greenstein VC, Zernant-Rajang J, et al. G1961E mutant allele in the Stargardt disease gene ABCA4 causes bull's eye maculopathy. *Exp Eye Res* 2009;89(1):16–24.
25. Allikmets R. A photoreceptor cell-specific ATP-binding transporter gene (ABCR) is mutated in recessive Stargardt macular dystrophy. *Nat Genet* 1997;17(1):122.
26. Cremers FP, van de Pol DJ, van Driel M, et al. Autosomal recessive retinitis pigmentosa and cone-rod dystrophy caused by splice site mutations in the Stargardt's disease gene ABCR. *Hum Mol Genet* 1998;7(3):355–362.
27. Martinez-Mir A, Paloma E, Allikmets R, et al. Retinitis pigmentosa caused by a homozygous mutation in the Stargardt disease gene ABCR. *Nat Genet* 1998;18(1):11–12.
28. Fishman GA, Stone EM, Eliason DA, Taylor CM, Lindeman M, Derlacki DJ. ABCA4 gene sequence variations in patients with autosomal recessive cone-rod dystrophy. *Arch Ophthalmol* 2003;121(6):851–855.
29. Klevering BJ, Yzer S, Rohrschneider K, et al. Microarray-based mutation analysis of the ABCA4 (ABCR) gene in autosomal recessive cone-rod dystrophy and retinitis pigmentosa. *Eur J Hum Genet* 2004;12(12):1024–1032.
30. Riveiro-Alvarez R, Aguirre-Lamban J, Lopez-Martinez MA, et al. Frequency of ABCA4 mutations in 278 Spanish controls: an insight into the prevalence of autosomal recessive Stargardt disease. *Br J Ophthalmol* 2009;93(10): 1359–1364.
31. Schindler EI, Nylen EL, Ko AC, et al. Deducing the pathogenic contribution of recessive ABCA4 alleles in an outbred population. *Hum Mol Genet* 2010;19(19):3693–3701.
32. Aguirre-Lamban J, Gonzalez-Aguilera JJ, Riveiro-Alvarez R, et al. Further associations between mutations and polymorphisms in the ABCA4 gene: clinical implication of allelic variants and their role as protector/risk factors. *Invest Ophthalmol Vis Sci* 2011;52(9):6206–6212.
33. Zernant J, Schubert C, Im KM, et al. Analysis of the ABCA4 gene by next-generation sequencing. *Invest Ophthalmol Vis Sci* 2011;52(11):8479–8487.
34. Robson AG, Egan CA, Luong VA, Bird AC, Holder GE, Fitzke FW. Comparison of fundus autofluorescence with photopic and scotopic fine-matrix mapping in patients with retinitis pigmentosa and normal visual acuity. *Invest Ophthalmol Vis Sci* 2004;45(11):4119–4125.
35. Sergouniotis PI, Davidson AE, Lenassi E, Devery SR, Moore AT, Webster AR. Retinal structure, function, and molecular pathologic features in gyrate atrophy. *Ophthalmology* 2012;119(3):596–605.
36. Sergouniotis PI, Holder GE, Robson AG, Michaelides M, Webster AR, Moore AT. High-resolution optical coherence tomography imaging in KCNV2 retinopathy. *Br J Ophthalmol* 2012;96(2):213–217.
37. Tsunoda K, Watanabe K, Akiyama K, Usui T, Noda T. Highly reflective foveal region in optical coherence tomography in eyes with vitreomacular traction or epiretinal membrane. *Ophthalmology* 2012;119(3):581–587.
38. Zweifel SA, Engelbert M, Laud K, Margolis R, Spaide RF, Freund KB. Outer retinal tubulation: a novel optical coherence tomography finding. *Arch Ophthalmol* 2009;127(12): 1596–1602.
39. Bach M, Brigell MG, Hawlina M, et al. ISCEV standard for clinical pattern electroretinography (PERG): 2012 update. *Doc Ophthalmol* 2013;126(1):1–7.
40. Marmor MF, Fulton AB, Holder GE, Miyake Y, Brigell M, Bach M. ISCEV standard for full-field clinical electroretinography (2008 update). *Doc Ophthalmol* 2009;118(1): 69–77.
41. Hood DC, Bach M, Brigell M, et al. ISCEV standard for clinical multifocal electroretinography (mfERG) (2011 edition). *Doc Ophthalmol* 2012;124(1):1–13.
42. Bellmann C, Neveu MM, Scholl HP, et al. Localized retinal electrophysiological and fundus autofluorescence imaging abnormalities in maternal inherited diabetes and deafness. *Invest Ophthalmol Vis Sci* 2004;45(7):2355–2360.
43. Jaakson K, Zernant J, Kulm M, et al. Genotyping microarray (gene chip) for the ABCR (ABCA4) gene. *Hum Mutat* 2003; 22(5):395–403.
44. Ng PC, Henikoff S. SIFT: predicting amino acid changes that affect protein function. *Nucleic Acids Res* 2003;31(13):3812–3814.
45. Adzhubei IA, Schmidt S, Peshkin L, et al. A method and server for predicting damaging missense mutations. *Nat Methods* 2010;7(4):248–249.
46. Allikmets R, Shroyer NF, Singh N, et al. Mutation of the Stargardt disease gene (ABCR) in age-related macular degeneration. *Science* 1997;277(5333):1805–1807.
47. Rozet JM, Gerber S, Souied E, et al. Spectrum of ABCR gene mutations in autosomal recessive macular dystrophies. *Eur J Hum Genet* 1998;6(3):291–295.
48. Lewis RA, Shroyer NF, Singh N, et al. Genotype/phenotype analysis of a photoreceptor-specific ATP-binding cassette transporter gene, ABCR, in Stargardt disease. *Am J Hum Genet* 1999;64(2):422–434.
49. Rivera A, White K, Stohr H, et al. A comprehensive survey of sequence variation in the ABCA4 (ABCR) gene in Stargardt disease and age-related macular degeneration. *Am J Hum Genet* 2000;67(4):800–813.
50. Birch DG, Peters AY, Locke KL, Spencer R, Megarity CF, Travis GH. Visual function in patients with cone-rod dystrophy (CRD) associated with mutations in the ABCA4 (ABCR) gene. *Exp Eye Res* 2001;73(6):877–886.
51. Briggs CE, Rucinski D, Rosenfeld PJ, et al. Mutations in ABCR (ABCA4) in patients with Stargardt macular

in the foveal-sparing phenotype compared to the typical phenotype; there was also clear concordance in sibships with the foveal-sparing phenotype, although a possible influence of genetic/environmental modifiers cannot be excluded.

The present study identifies distinct clinical features and molecular findings in patients with Stargardt disease and foveal sparing. It has highlighted that this phenotype is associated with a later onset of disease, better visual acuity (≥0.48 logMAR), often normal full-field ERGs, and evidence of outer retinal tubulation. These data assist genetic counseling and may help in the appropriate selection of patients for therapeutic clinical trials for *ABCA4* retinopathy.

ALL AUTHORS HAVE COMPLETED AND SUBMITTED THE ICMJE FORM FOR DISCLOSURE OF POTENTIAL CONFLICTS OF INTEREST and none were reported. Publication of this article was supported by grants from the National Institute for Health Research Biomedical Research Centre at Moorfields Eye Hospital National Health Service Foundation Trust and University College London, Institute of Ophthalmology (London, United Kingdom); Fight For Sight (London, United Kingdom); Moorfields Eye Hospital Special Trustees (London, United Kingdom); Macular Disease Society (London, United Kingdom); the Foundation Fighting Blindness (Columbia, Maryland, USA); Suzuken Memorial Foundation (Nagoya, Aichi, Japan); Mitsukoshi Health and Welfare Foundation (Tokyo, Japan), Daiwa Anglo-Japanese Foundation (Tokyo, Japan); and Grant-in-Aid for Young Scientists (B) of the Ministry of Education, Culture, Sports, Science and Technology (Tokyo, Japan). Contributions of authors: conception and design (K.F., A.M., M.M., A.W.); analysis and interpretation (K.F., P.S., A.D., K.Tsunoda, K.Tsubota, A.R., A.M., G.H., M.M., A.W.); writing the article (K.F., P.S., A.D., G.W., R.C., C.E., A.R., A.M., G.H., M.M., A.W.); critical revision of the article (K.F., P.S., A.D., A.R., A.M., G.H., M.M., A.W.); final approval of the article (K.F., P.S., A.D., A.R., A.M., G.H., M.M., A.W.); data collection (K.F., A.D., G.W., R.C., C.E., A.R., A.M., G.H., M.M., A.W.); provision of materials, patients, or resources (K.F., G.W., R.C., C.E., A.M., M.M., A.W.); statistical expertise (K.F., K.Tsunoda, K.Tsubota, M.M.); obtaining funding (K.F., K.Tsunoda, K.Tsubota, A.M., M.M., A.W.); literature search (K.F., P.S., A.D., A.M., M.M., A.W.); and administrative, technichal, or logistic support (K.F., A.M., M.M., A.W.).

The authors are grateful to those who contributed to the assembly of the *ABCA4* panel, particularly Naushin Waseem, Bev Scott, and Sophie Devery (University College London, Institute of Ophthalmology, London, UK). We thank Professor Yozo Miyake (Aichi Medical University, Aichi, Japan), Catey Bunce, Rajarshi Mukerjee, Arundhati Dev Borman, Eva Lenassi, and Aman Chandra (University College London, Institute of Ophthalmology, London, UK) for their insightful comments.

REFERENCES

1. Stargardt K. Uber familiare progressive degeneration in der makulagegend des auges. *Albrecht von Grafes Arch Klin Ophthalmol* 1909;71:534–550.
2. Allikmets R, Singh N, Sun H, et al. A photoreceptor cell-specific ATP-binding transporter gene (ABCR) is mutated in recessive Stargardt macular dystrophy. *Nat Genet* 1997; 15(3):236–246.
3. Michaelides M, Hunt DM, Moore AT. The genetics of inherited macular dystrophies. *J Med Genet* 2003;40(9): 641–650.
4. Burke TR, Tsang SH. Allelic and phenotypic heterogeneity in ABCA4 mutations. *Ophthalmic Genet* 2011;32(3):162–174.
5. Rotenstreich Y, Fishman GA, Anderson RJ. Visual acuity loss and clinical observations in a large series of patients with Stargardt disease. *Ophthalmology* 2003;110(6):1151–1158.
6. Fujinami K, Akahori M, Fukui M, Tsunoda K, Iwata T, Miyake Y. Stargardt disease with preserved central vision: identification of a putative novel mutation in ATP-binding cassette transporter gene. *Acta Ophthalmol* 2011;89(3):297–298.
7. Armstrong JD, Meyer D, Xu S, Elfervig JL. Long-term follow-up of Stargardt's disease and fundus flavimaculatus. *Ophthalmology* 1998;105(3):448–458.
8. Fishman GA, Stone EM, Grover S, Derlacki DJ, Haines HL, Hockey RR. Variation of clinical expression in patients with Stargardt dystrophy and sequence variations in the ABCR gene. *Arch Ophthalmol* 1999;117(4):504–510.
9. Lois N, Holder GE, Bunce C, Fitzke FW, Bird AC. Phenotypic subtypes of Stargardt macular dystrophy-fundus flavimaculatus. *Arch Ophthalmol* 2001;119(3):359–369.
10. Yatsenko AN, Shroyer NF, Lewis RA, Lupski JR. Late-onset Stargardt disease is associated with missense mutations that map outside known functional regions of ABCR (ABCA4). *Hum Genet* 2001;108(4):346–355.
11. McBain VA, Townend J, Lois N. Progression of retinal pigment epithelial atrophy in stargardt disease. *Am J Ophthalmol* 2012;154(1):146–154.
12. Westeneng-van Haaften SC, Boon CJ, Cremers FP, Hoefsloot LH, den Hollander AI, Hoyng CB. Clinical and genetic characteristics of late-onset Stargardt's disease. *Ophthalmology* 2012;119(6):1199–1210.
13. Testa F, Rossi S, Sodi A, et al. Correlation between photoreceptor layer integrity and visual function in patients with Stargardt disease: implications for gene therapy. *Invest Ophthalmol Vis Sci* 2012;53(8):4409–4415.
14. Lenassi E, Jarc-Vidmar M, Glavac D, Hawlina M. Pattern electroretinography of larger stimulus field size and spectral-domain optical coherence tomography in patients with Stargardt disease. *Br J Ophthalmol* 2009;93(12):1600–1605.
15. Gomes NL, Greenstein VC, Carlson JN, et al. A comparison of fundus autofluorescence and retinal structure in patients with Stargardt disease. *Invest Ophthalmol Vis Sci* 2009;50(8): 3953–3959.
16. Lazow MA, Hood DC, Ramachandran R, et al. Transition zones between healthy and diseased retina in choroideremia (CHM) and Stargardt disease (STGD) as compared to retinitis pigmentosa (RP). *Invest Ophthalmol Vis Sci* 2011; 52(13):9581–9590.
17. Genead MA, Fishman GA, Anastasakis A. Spectral-domain OCT peripapillary retinal nerve fibre layer thickness measurements in patients with Stargardt disease. *Br J Ophthalmol* 2011;95(5):689–693.
18. Chen Y, Ratnam K, Sundquist SM, et al. Cone photoreceptor abnormalities correlate with vision loss in patients with Stargardt disease. *Invest Ophthalmol Vis Sci* 2011;52(6):3281–3292.

TABLE 4. Comparison of the Most Prevalent *ABCA4* Variants' Frequency Between the Cohort With the Foveal-Sparing Stargardt Disease and the Group With the Typical Stargardt Disease (Without Evidence of Foveal Sparing)

	Number of Alleles and Those Frequencies	
	Foveal-Sparing Stargardt Disease (n = 31, Total 30 Variants in 62 Alleles)	Typical Stargardt Disease (n = 140, Total 72 Variants in 280 Alleles)
c.2588G>C, p.Gly863Ala	4 (6.45%)	19 (6.79%)
c.4139C>T, p.Pro1380Leu	2 (3.23%)	14 (5.00%)
c.6079C>T, p.Leu2027Phe	4 (6.45%)	10 (3.57%)
c.6089G>A, p.Arg2030Gln	4 (6.45%)	3 (1.07%)
c.5461-10T>C	3 (4.84%)	23 (8.21%)
c.5882G>A, p.Gly1961Glu	1 (1.61%)	17 (6.07%)

p. Pro1380Leu, c.5461-10T>C, and p.Gly1961Glu, occurring in 19, 14, 23, and 17 patients, respectively. Sequence variant frequencies were compared between the 2 groups of patients and there was a suggestion of a higher frequency of the variant p.Arg2030Gln in the cohort with the foveal-sparing phenotype compared to the group with typical Stargardt disease (Table 4).

DISCUSSION

THIS REPORT DESCRIBES THE DETAILED CLINICAL AND molecular genetic characteristics of 40 patients with Stargardt disease and foveal sparing on AF imaging; at least 1 disease-causing *ABCA4* allele was identified in 78% of subjects.

The median age of onset was 43.5 years, with a median visual acuity of 0.18, and 13 patients (32%) were asymptomatic, in keeping with previous reports.[5,6,12,22] Thirty-eight of 40 patients (98%) had logMAR visual acuity better than or equal to 0.48, with the remaining 2 subjects also having a visual acuity better than or equal to 0.48 at the initial consultation. Unsurprisingly, the normal AF signal at the fovea is strongly associated with relative visual acuity preservation.

Four previously reported fundus patterns were identified, with 22 patients (55%) showing patchy parafoveal atrophy surrounded by numerous yellow-white flecks in our cohort.[5,12] The median age of onset and median visual acuity associated with each pattern did not differ significantly. These findings suggest that late presentation of disease and preserved visual acuity are characteristic features of the foveal-sparing phenotype, whereas it may be associated with a variable fundus appearance.

Morphologic preservation of foveal structure was present in SDOCT in most cases. The 6 patients with foveal thinning (less than 100 μm central foveal thickness) also had more severe visual acuity loss (0.48) and a longer duration of disease (12.8 years). Evidence of outer retinal tubulation was identified in 15 of 33 patients (45%). Outer retinal tubulation is believed to occur in response to RPE loss/dysfunction, since these rosettes may represent degenerating photoreceptor cells becoming arranged in a circular or ovoid fashion to promote survival.[35,38] The high incidence of outer retinal tubulation in the foveal-sparing phenotype cohort is in keeping with predominant RPE cell failure in the foveal-sparing phenotype of Stargardt disease.[35,38]

In consideration of the electrophysiological findings, the majority (67%) of patients were in ERG group 1 (localized macular dysfunction with normal ERG). It is, however, noteworthy that 8 of 33 subjects (24%) were in ERG group 3 (macular dysfunction and additional generalized cone and rod dysfunction), indicating that foveal sparing can occur even in the context of generalized retinal dysfunction.

Perimetry data were not collected on this cohort. Although some data are available on foveal-sparing patients,[6,12] more detailed analysis on a larger group of patients early in the disorder would be informative. This might determine the specific region of the macula where dysfunction starts and, if scotopic and photopic thresholds are measured separately, the relative vulnerability of rod and cone systems.

Thirty likely disease-causing variants were identified in 31 patients, including 29 previously reported disease-causing variants and the 1 novel putative disease-causing splice site variant, c.1760+1G>T.[8,20,46–54] Interestingly, there was a suggestion of a higher frequency of the substitution p.Arg2030Gln in the foveal-sparing cohort (incidence ratio: 6.5% for the foveal-sparing phenotype and 1.1% for typical Stargardt), with a possible lower incidence of p.Gly1961Glu in the foveal-sparing cohort (incidence ratio: 1.6% for the foveal-sparing phenotype and 6.1% for typical Stargardt). Although these molecular differences did not meet statistical significance, larger cohorts of patients will help to establish their importance. Typical Stargardt disease is characterized by early foveal cone failure, in direct contrast to the foveal-sparing phenotype, suggesting that there may be more than 1 mechanism influencing cell death, which could either relate to the specific sequence variant or other genetic/environmental modifiers. In support of a direct genotype-phenotype association, a different preponderance of variants was identified

TABLE 3. Allele Frequencies of 72 *ABCA4* Variants Identified in a Comparison Group[a] With the Typical Stargardt Disease (140 Patients Without Evidence of Foveal Sparing on Autofluorescence Imaging)

Exon	Nucleotide Substitution and Amino Acid Change	Number of Alleles	Allele Frequency
2	c.71G>A, p.Arg24His	1	0.36%
2	c.161G>A, p.Cys54Tyr	3	1.07%
3	c.223T>G, p.Cys75Gly	1	0.36%
5	c.455G>A, p.Arg152Gln	1	0.36%
5	c.454C>T, p.Arg152*	1	0.36%
5	c.466 A>G, p.Ile156Val	2	0.71%
6	c.634C>T, p. Arg212Cys	3	1.07%
6	c.656G>C, p.Arg219Thr	1	0.36%
6	c.666_678delAAAGACGGTGCGC, p.Lys223_Arg226delfs	2	0.71%
6	c.768G>T, Splicing site	4	1.42%
8	c.1037A>C, p.Lys346Thr	1	0.36%
10	c.1222C>T, p.Arg408*	3	1.07%
12	c.1622T>C, p.Leu541Pro	2	0.71%
12	c.1648 G>T, p.Gly550*	1	0.36%
13	c.1804C>T, p.Arg602Trp	1	0.36%
13	c.1817G>A, p.Gly606Asp	1	0.36%
13	c.1922G>C, p.Cys641Ser	1	0.36%
Int 13	c.1937+1G>A, Splicing site	2	0.71%
14	c.1957C>T, p.Arg653Cys	2	0.71%
17	c.2588G>C, p.Gly863Ala	19	6.79%
18	c.2701A>G, p.Thr901Ala	1	0.36%
19	c.2791G>A, p.Val931Met	2	0.71%
19	c.2894A>G, p.Asn965Ser	1	0.36%
20	c.2966T>C, p.Vla989Ala	3	1.07%
20	c.2971G>C, p.Gly991Arg	2	0.71%
21	c.3056C>T, p.Thr1019Met	1	0.36%
21	c.3113C>T, p.Ala1038Val	3	1.07%
21	c.3064G>A, p.Glu1022Lys	2	0.71%
22	c.3211_3212insGT, p.Ser1071Cysfs	6	2.14%
22	c.3259G>A, p.Glu1087Lys	4	1.43%
22	c.3292C>T, p.Arg1098Cys	1	0.36%
22	c.3322C>T, p.Arg1108Cys	5	1.79%
22	c.3323G>A, p.Arg1108His	1	0.36%
23	c.3364G>A, p.Glu1122Lys	1	0.36%
23	c.3386G>A, p.Arg1129His	1	0.36%
24	c.3602T>G, p.Leu1201Arg	3	1.07%
27	c.3898C>T, p.Arg1300*	2	0.71%
28	c.4139C>T, p.Pro1380Leu	14	5.00%
28	c.4222T>C, p.Trp1408Arg	1	0.36%
28	c.4234C>T, p.Gly1412*	1	0.36%
28	c.4253+5G>T, Splice site	1	0.36%
28	c.4253+4C>T, Splice site	1	0.36%
29	c.4283C>T, p.Thr1428Met	1	0.36%
29	c.4319T>C, p.Phe1440Ser	1	0.36%
29	c.4462T>C, p.Cys1488Arg	1	0.36%
30	c.4469G>A, p.Cys1490Tyr	5	1.79%
30	c.4537_4538insC, p.Gly1513Profs	1	0.36%
31	c.4577C>T, p.Thr1526Met	2	0.71%
33	c.4715C>T, p.Thr1572Met	1	0.36%

Continued on next page

TABLE 3. Allele Frequencies of 72 ABCA4 Variants Identified in a Comparison Groupa With the Typical Stargardt Disease (140 Patients Without Evidence of Foveal Sparing on Autofluorescence Imaging) *(Continued)*

Exon	Nucleotide Substitution and Amino Acid Change	Number of Alleles	Allele Frequency
Int 33	c.4773+48C>T	1	0.36%
34	c.4793C>A, p.Ala1598Asp	1	0.36%
35	c.c.4918C>T, p.Arg1640Trp	1	0.36%
Int 35	c.5018+2T>C, Splice site	2	0.71%
36	c.5114G>A, p.Arg1705Gln	2	0.71%
37	c.5222_5233delTGGTGGTGGGC, p.Lys1741Hisfs	1	0.36%
37	c.5281_5289delCTT CCT GCC, p.Pro1761_Leu1763del	2	0.71%
Int 38	c.5461-10T>C	23	8.21%
Int 39	c.5585-1G>A, Splice site	1	0.36%
Int 40	c.5714+5G>A, Splice site	5	1.79%
42	c.5882G>A, p.Gly1961Glu	17	6.07%
43	c.5908C>T, p.Leu1970Phe	2	0.71%
43	c.5917delG, p.Val1973*	1	0.36%
44	c.6079C>T, p.Leu2027Phe	10	3.57%
44	c.6089G>A, p.Arg2030Gln	3	1.07%
44	c.6118C>T, p.Arg2040*	1	0.36%
45	c.6148G>C, p.Val2050Leu	3	1.43%
46	c.6286G>A, p.Glu2096Lys	1	0.36%
46	c.6320G>A, p.Arg2107His	4	1.43%
47	c.6445C>T, p.Arg2149*	1	0.36%
47	c.6449G>A, p.Cys2150Tyr	3	1.07%
48	c.6658C>T, p.Gln2220*	3	1.07%
48	c.6709_6710insG, p.Thr2237Serfs	1	0.36%

Int = Intron.

[a]The comparison group consisted of all patients without evidence of foveal sparing on autofluorescence imaging and also harbored at least 1 *ABCA4* disease-causing variant following screening with the arrayed primer extension microarray. One hundred and forty subjects from a total cohort of 438 individuals fulfilled these criteria.

and 1 uncertain effect (c.5461-10T>C); and 23 non-null variants (Table 2). Twenty-nine previously reported disease-causing variants and 1 novel putative disease-causing variant were identified (c.1760+1G>T). The most common variants identified were p.Gly863Ala, c.5461-10T>C, p.Leu2027Phe, and p.Arg2030Gln, occurring, respectively, in 4, 3, 3, and 4 patients with the foveal-sparing phenotype of Stargardt disease. One patient was identified to be homozygous for the p.Leu2027Phe variant; none had 2 or more null variants.

Molecular genetic data for the 140 individuals with typical Stargardt disease (without foveal sparing / with foveal atrophy) are summarized in Table 3. Seventy-two likely disease-causing variants were identified: 23 null variants, including 7 predicted to affect splicing; and 49 non-null variants. The 4 most prevalent variants were p.Gly863Ala,

TABLE 2. Investigation of the Pathogenicity of *ABCA4* Variants Identified in 40 Patients With the Foveal-Sparing Phenotype of Stargardt Disease

					SIFT*		Polyphen 2†		HSF Matrix‡						
Exon	Nucleotide Substitution and Amino Acid Change	Number of Alleles	Het/Homo	Previous Report	Pred.	Index (0-1)	Pred.	Hum Var Score (0-1)	Site Affected	Wt CV	Mt CV	CV % Variation	Allelic Frequency Observed by EVS§	Reference
2	c.71G>A, p.Arg24His	1	Het	Lewis[18]	Tol.	NA	PRD	0.98				No change	ND	
6	c.768G>T, Splice site	1	Het	Klevering[20]	Tol.	0.56	NA		Donor	70.4	58	Site broken (−17.51)	ND	
6	c.658C>T, p.Arg220Cys	1	Het	Webster[53]	Tol.	NA	Benign	0.39				No change	ND	
11	c.1411G>A, p.Glu471Lys	1	Het	Allikmets[46]	Tol	NA	Benign	0.01	Acceptor	71.7	43	Site broken (−40.4)	11/13006	db SNP (rs1800548)
12	c.1622T>C, p.Leu541Pro	1	Het	Fishman[8]	Intol.	0.00	PRD	0.961				No change	2/13006	db SNP (rs61751392)
Int 12	c.1760+1G>T, Splice site	1	Het	This study	NA		NA		Donor	84.6	58	WT site broken (−31.72)	ND	
13	c.1805G>A, p.Arg602Gln	2	Het	Webster[53]	Tol.	NA	PRD	0.513		48.9	78	New site (+59.14)	2/13006	db SNP (rs61749410)
14	c.1957C>T, p.Arg653Cys	2	Het	Rivera[49]	Tol.	0.10	PRD	0.999				No change	ND	
17	c. 2588G>C, p.Gly863Ala	4	Het	Allikmets[46]	Intol.	0.01	PRD	0.996				No change	68/13006	db SNP (rs76157638)
21	c.3113C>T, p.Ala1038Val	1	Het	Webster[53]	Tol.	NA	Benign	0.014	Donor	43.5	70	New site (+61.72)	22/13006	db SNP (rs61751374)
24	c.3602T>G, p.Leu1201Arg	2	Het	Lewis[18]	Tol.	NA	Benign	0.052	Donor	61.3	74	New site (+20.08)	416/13006	db SNP (rs61750126)
27	c.3898C>T, p.Arg1300*	1	Het	Rivera[49]	NA		NA						ND	
28	c.4139C>T, p.Pro1380Leu	2	Het	Lewis[18]	Intol.	0.01	Benign	0.377				No change	2/13006	db SNP (rs61750130)
28	c.4222 T>C, p.Trp1408Arg	2	Het	Lewis[18]	Tol.	NA	PRD	0.845				No change	ND	dbSNP (rs61750135)
29	c.4319T>C, p.Phe1440Ser	1	Het	Lewis[18]	Tol.	NA	PRD	0.744				No change	ND	dbSNP (rs61750141)
30	c.4469G>A, p.Cys1490Tyr	1	Het	Webster[53]	Intol.	0.03	PRD	0.994				No change	ND	dbSNP (rs61751402)
31	c.4577C>T, p.Thr1526Met	1	Het	Lewis[18]	Intol.	0.00	PRD	0.91				No change	ND	db SNP (rs61750152)
31	c.4594G>T, p.Asp1532Asn	3	Het	Lewis[18]	Tol.	NA	PRD	0.853				No change	ND	
33	c.4685T>C, p.Ile1562Thr	1	Het	Allikmets[46]	Tol.	NA	Benign	0.034				No change	18/13006	db SNP (rs1762111)
35	c.4956T>G, p.Tyr1652*	1	Het	Fumagalli[52]	NA		NA		Acceptor	43	72	New site (+67.36)	ND	
35	c.4918C>T, p.Arg1640Trp	2	Het	Rozet[47]	Intol.	0.00	PRD	1				No change	ND	dbSNP (rs61751404)
35	c.4926C>G, p.Ser1642Arg	1	Het	Birch[50]	Tol.	0.68	Benign	0.116				No change	ND	db SNP (rs61753017)
Int 35	c.5018+2T>C, Splice site	1	Het	Fumagalli[52]	NA		NA		Donor	81.2	54	WT site broken (−33.07)	ND	
Int 38	c.5461-10T>C	3	Het	Briggs[50]	NA		NA					No change	3/13006	db SNP (rs1800728)
40	c.5693G>A, p.Arg1898His	2	Het	Allikmets[46]	NA		Benign	0.00				No change	25/13006	db SNP (rs1800552)
42	c.5882G>A, p.Gly1961Glu	1	Het	Allikmets[46]	Tol.	0.18	PRD	1				No change	41/13006	db SNP (rs1800553)
44	c.6079C>T, p.Leu2027Phe	4	Homo	Lewis[18]	Intol.	0.02	PRD	0.999				No change	4/13006	db SNP (rs61751408)
44	c.6089G>A, p.Arg2030Gln	4	Het	Lewis[18]	Tol.	NA	PRD	0.995				No change	8/13006	db SNP (rs61750641)
44	c.6118C>T, p.Arg2040*	1	Het	Rosenberg[54]	NA		NA						ND	
46	c.6320G>A, p.Arg2107His	1	Het	Fishman[8]	Intol.	0.00	PRD	0.996				No change	91/13006	db SNP (rs62642564)

EVS = Exome Variant Server; HSF = Human Splicing Finder program; Hum var score = Human var score; Int = intron; Intol = intolerant; Mt CV = mutant consensus value; NA = not applicable; ND = not detected; PRD = probably damaging; Pred. = prediction; SIFT = Sorting Intolerant from Tolerance program; Tol. = tolerant; Wt CV = wild-type consensus value.

*SIFT (version 4.0.4) results are reported to be tolerant if tolerance index >0.05 or intolerant if tolerance index <0.05. PolyPhen-2 (version 2.1) appraises mutations qualitatively as Benign, Possibly Damaging, or Probably Damaging based on the model's false-positive rate. The cDNA is numbered according to Ensemble transcript ID ENST00000370225, in which β1 is the A of the translation start codon. Human Splicing Finder (HSF, version 2.4.1) reports the results from the HSF matrix: the higher the consensus value, the stronger the predicted splice site. The values for the wild-type and mutant sequences are shown; the larger the difference between these values, the greater the chance that the variant can affect splicing. Minor allele frequency for each allele was estimated with reference to the EVS (NHLBI Exome Sequencing Project, Seattle, Washington, USA).

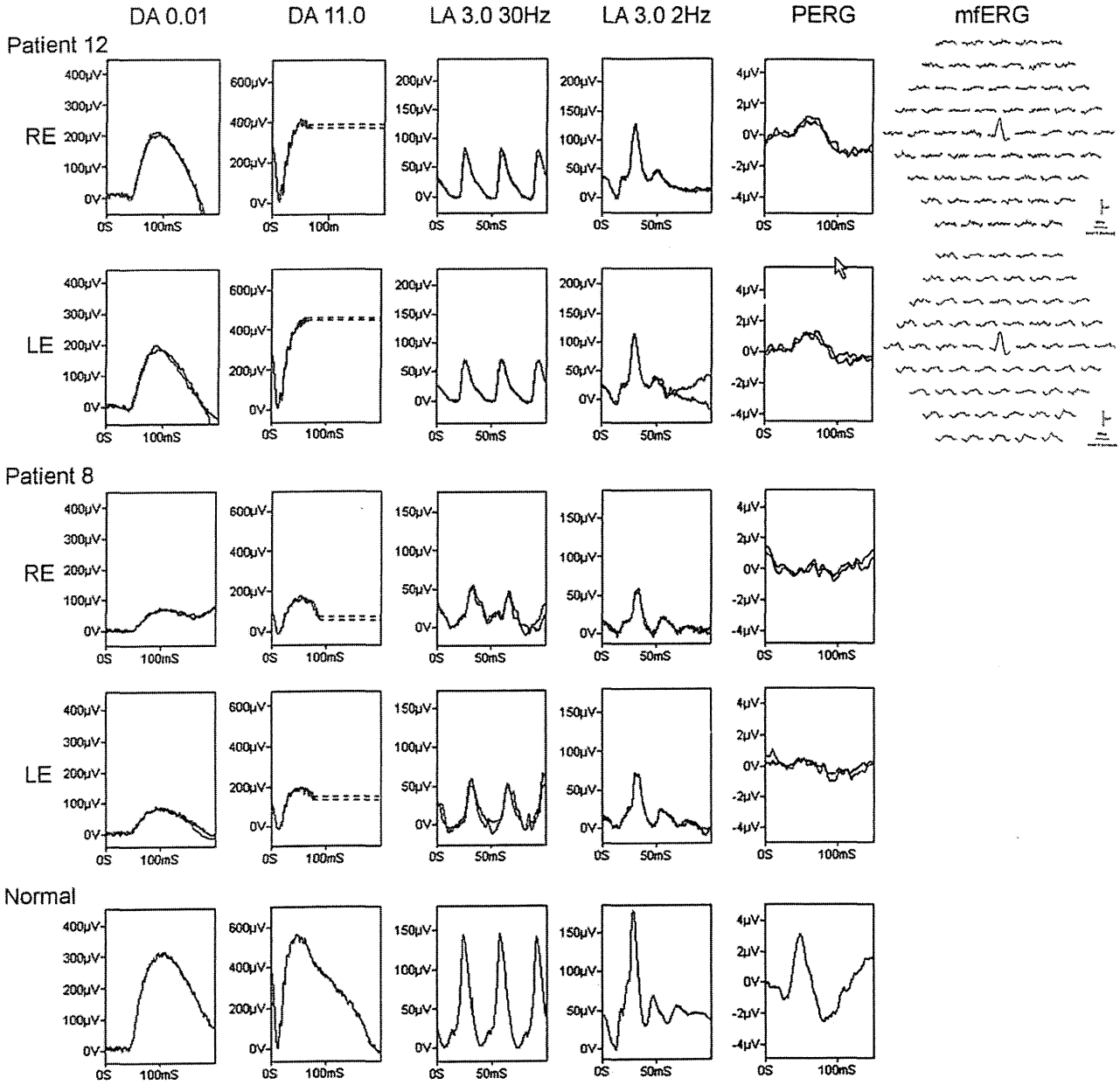

FIGURE 5. Full-field electroretinograms, pattern electroretinograms, and multifocal electroretinograms from 2 representative cases with the foveal-sparing phenotype of Stargardt disease, showing localized spared foveal function and marked macular dysfunction with generalized rod and cone system involvement, respectively (Patients 12 and 8). Full-field electroretinograms (ERGs) included: (1) dark-adapted dim flash 0.01 candela-seconds per square meter ($cd \cdot s \cdot m^{-2}$) (DA 0.01); (2) dark-adapted bright flash 11.0 $cd \cdot s \cdot m^{-2}$ (DA 11.0); (3) light-adapted 3.0 $cd \cdot s \cdot m^{-2}$ 30 Hz flicker (LA 3.0 30 Hz); and (4) light-adapted 3.0 $cd \cdot s \cdot m^{-2}$ at 2 Hz (LA 3.0 2 Hz). Patient 12 demonstrates normal ERGs and subnormal P50 components of pattern electroretinogram (PERG), consistent with macular dysfunction; multifocal electroretinograms (mfERGs) reveal sparing of localized foveal function with severe paracentral macular dysfunction bilaterally. Patient 8 has abnormal ERGs, consistent with generalized rod and cone system dysfunction, with marked PERG P50 reduction indicating marked macular involvement. Normal traces are shown for comparison.

The electrophysiological findings are summarized in Table 1; representative traces appear in Figure 5.

• MOLECULAR GENETICS: Likely disease-causing *ABCA4* variants were detected in 31 of 40 patients: 2 or more variants were identified in 16 patients and 1 variant in 15 subjects (Table 1). Detailed results, including in silico analysis to assist in the prediction of pathogenicity of the variants, are shown in Table 2. Thirty variants were found in 31 patients: 7 null variants, with 3 predicted to affect splicing

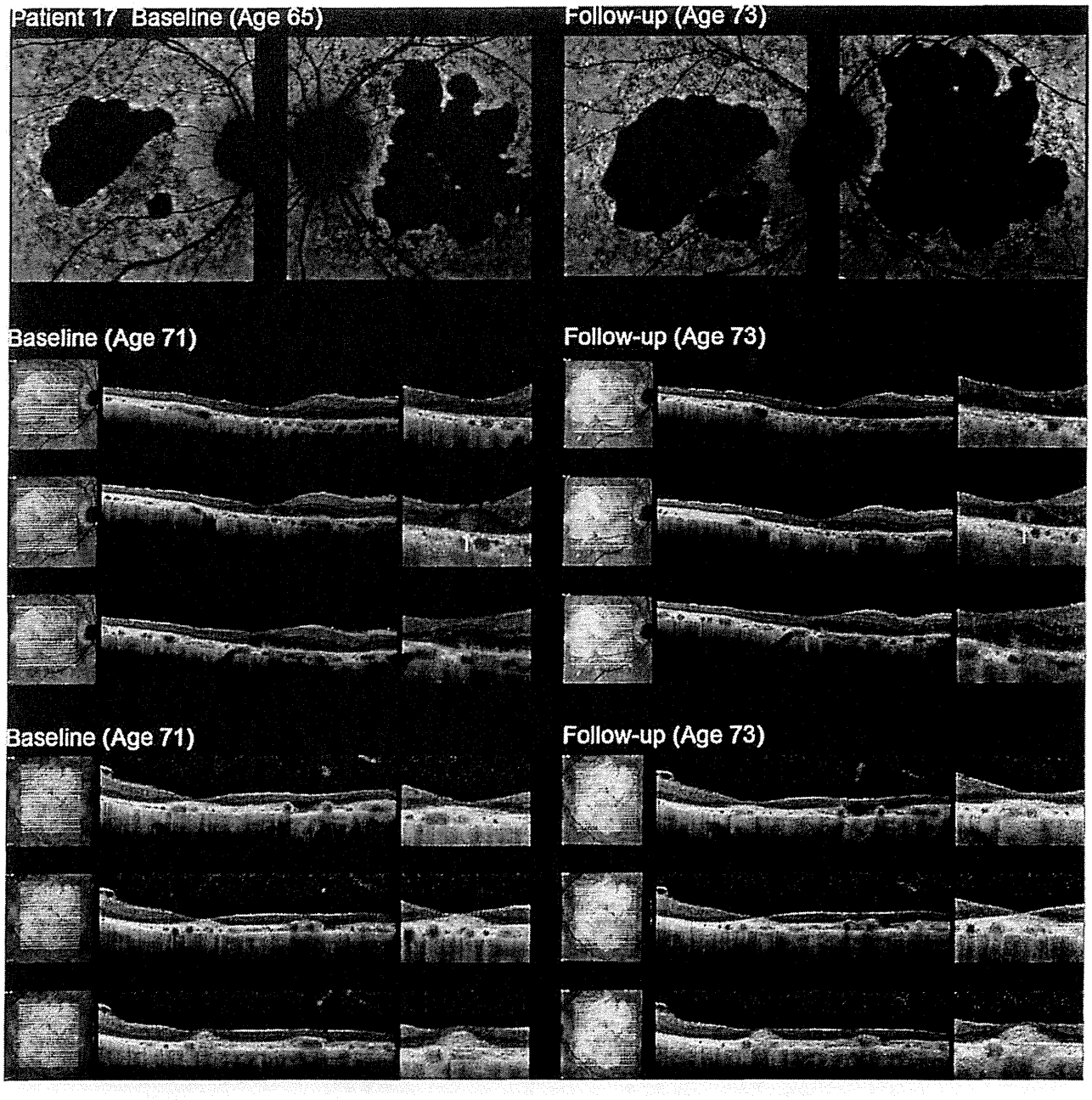

FIGURE 4. Serial autofluorescence and spectral-domain optical coherence tomographic images of Patient 17, with the foveal-sparing phenotype of Stargardt disease, illustrating enlargement of atrophy and progression of a snowball-like lesion to a recognizable outer retinal tubulation. Autofluorescence images at baseline show multiple patchy asymmetrical atrophic lesions in each eye. LogMAR visual acuity was −0.08 in the right eye but 1.0 in the left eye at baseline. Enlargement of the areas of atrophy occurs over time, with relative preservation of the foveal autofluorescence signal in the right eye (logMAR visual acuity 0.18). Disruption of outer retinal structure, with a snowball-like lesion (arrow) at the fovea in the right eye and foveal atrophy in the left eye, is present in baseline optical coherence tomographic images. The snowball-like lesion progresses over time, with outer retinal tubulation clearly present at follow-up in the right eye.

eyes of 3 patients (9%), abnormal responses in either eye of 16 subjects (48%), and undetectable responses in either eye of 14 individuals (42%). The median PERG P50 amplitude of PERG was 0.5 μV (range, 0.0-3.6 μV). The mfERG showed preservation of the response to the central hexagon surrounded by reduced responses to the paracentral hexagons in 3 of 8 patients (38%). These 3 patients had normal full-field ERGs. Five of 8 subjects (62%) had severely reduced central and paracentral responses, including 2 with normal ERGs and 3 with the group 3 ERG phenotype.

FIGURE 3. Serial autofluorescence and spectral-domain optical coherence tomographic images of Patient 9, with the foveal-sparing phenotype of Stargardt disease, showing increasing of atrophy and architectural disruption. Patient 9 presented without any visual symptoms 5 years prior to the most recent examination. LogMAR visual acuity was 0.0 in each eye. Autofluorescence images show numerous foci of high or low signal at the posterior pole at baseline, with increasing atrophy over time. Optical coherence tomographic images at baseline show relatively preserved foveal structure with an intact junction between the inner and outer photoreceptor segments (IS/OS) in each eye; IS/OS disruption is present at follow-up examination.

Fifteen patients (45%) showed evidence of outer retinal tubulation. The median age of onset and the mean duration of disease of these 15 patients with outer retinal tubulation were 45.0 and 7.2 years, compared to 43.0 and 2.1 years for the 18 subjects without outer retinal tubulation. The median visual acuity was the same in both groups. AF and SDOCT images of 2 representative cases (Patients 9 and 17) demonstrate slow progression over time (Figures 3 and 4).

Electrophysiological assessment was performed in 33 patients. ERG and PERG were recorded in all; mfERG was obtained in 8 individuals. Twenty-two of the 33 patients (67%) were in ERG group 1, 3 (9%) in ERG group 2, and 8 (24%) in ERG group 3. PERG was normal in both

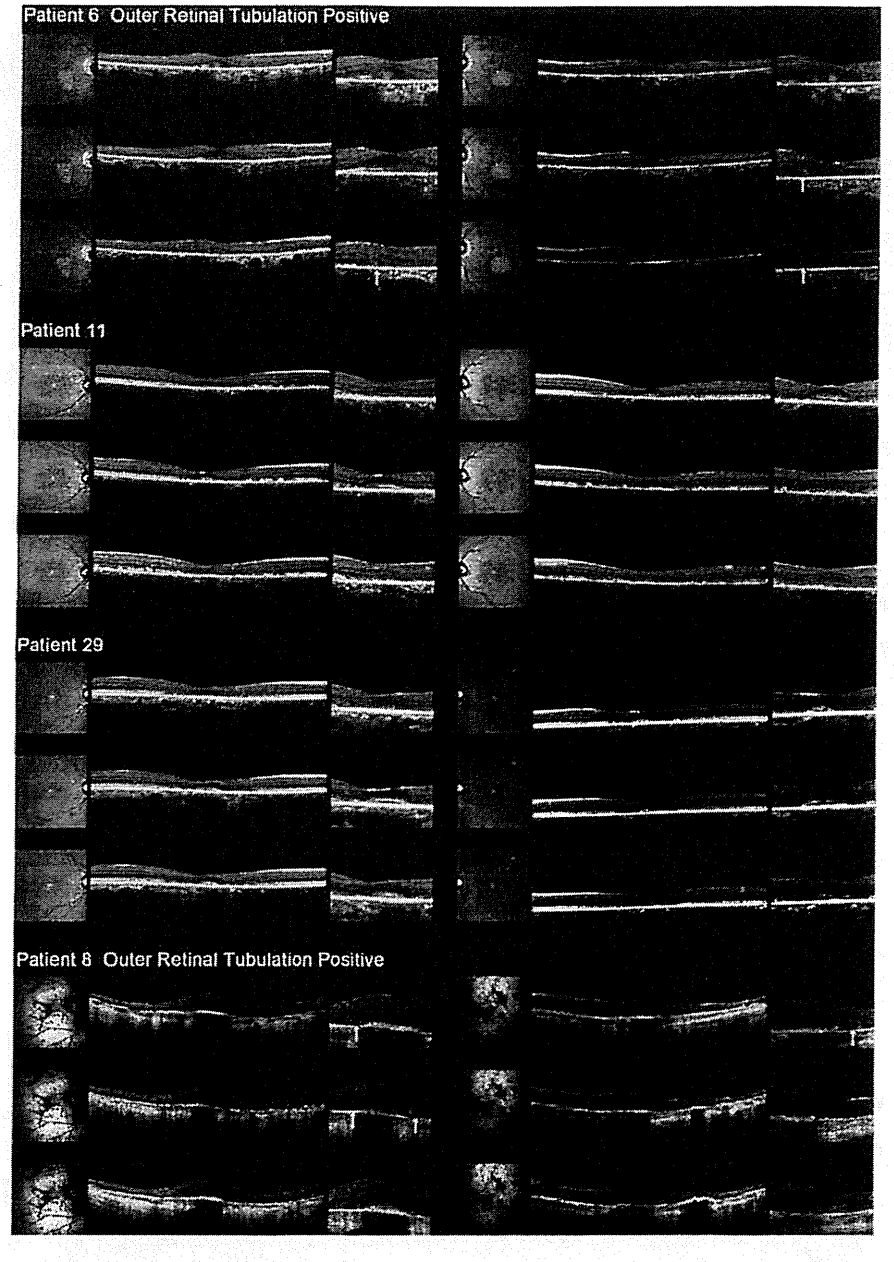

FIGURE 2. Spectral-domain optical coherence tomographic images of the 4 representative cases with the foveal-sparing phenotype of Stargardt disease illustrated in Figure 1 (Patients 6, 11, 29, and 8), demonstrating relatively preserved foveal structure and outer retinal tubulation. There is relatively preserved foveal structure in all 4 patients, with 2 showing outer retinal tubulation (Patients 6 and 8). Arrows in the magnified images identify outer retinal tubulation.

RPE changes and/or localized parafoveal yellow-white flecks; and pattern 4 (n = 2, 5%) had multiple patchy atrophic lesions, extending beyond the arcades. One patient (2.5%) had a bull's-eye maculopathy (Patient 33). These data are summarized in Table 1. The median ages of onset of patterns 1, 2, 3, and 4 were 46.0, 39.5, 36.0, and 43.5 years, respectively; the mean duration of disease was 5.1, 0.1, 2.9, and 15.0 years. The median logMAR visual acuity of patterns 1, 2, 3, and 4 was 0.18, 0.00, 0.18, and 0.05, respectively. Color fundus photographs and AF images of 4 representative cases are shown in Figure 1, with associated OCT images in Figure 2.

SDOCT images were obtained in 33 individuals (Table 1). The median central foveal thickness of the right and left eyes was 180.0 μm and 185.0 μm, respectively (range, 32-219 μm and 39-273 μm). The median central foveal thickness for each fundus pattern in the right eye was 179.5 μm for pattern 1 (18 patients); 223.5 μm for pattern 2 (6 subjects); 159.5 μm for pattern 3 (6 individuals); and 216.0 μm for pattern 4 (2 patients).

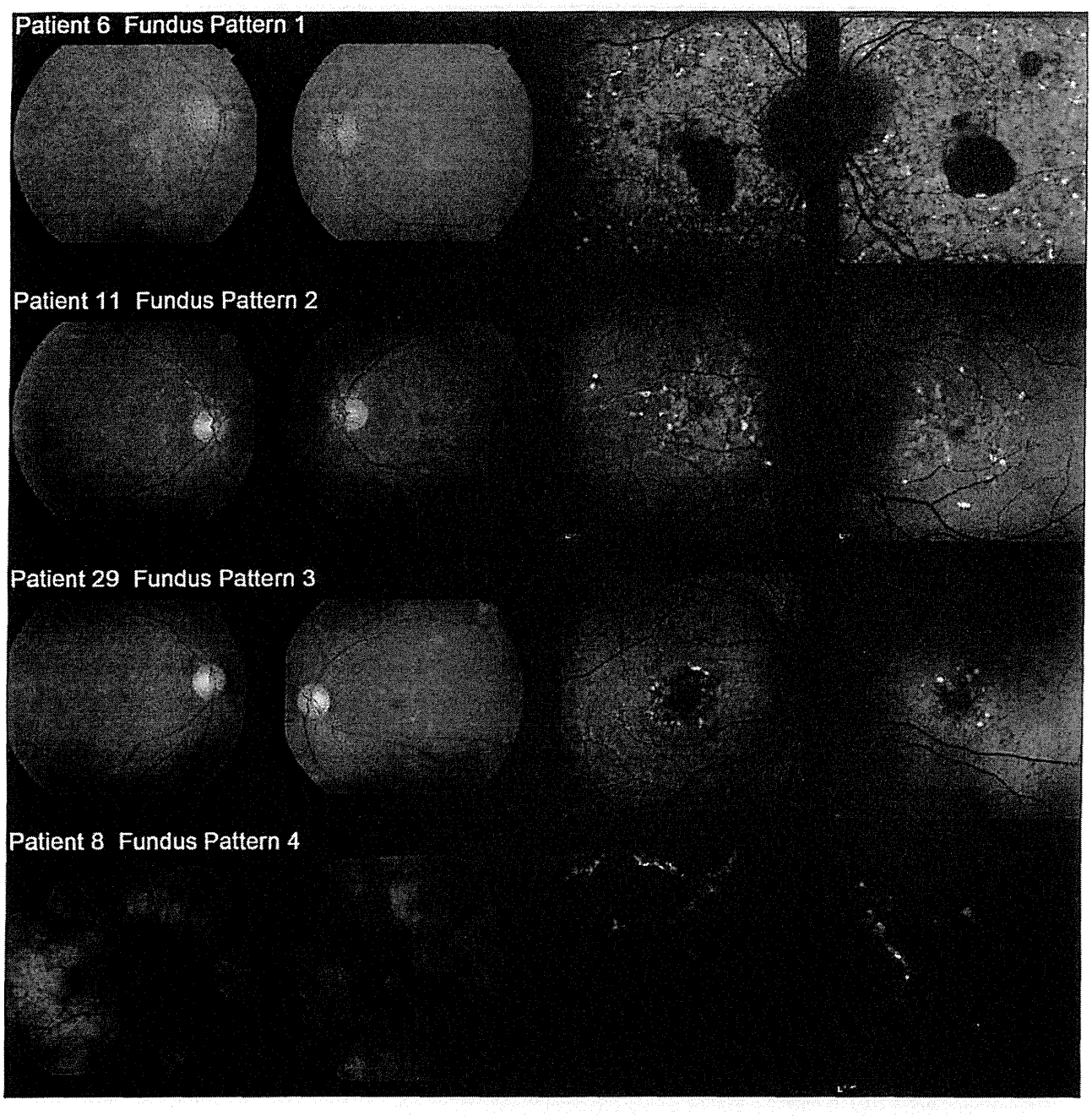

FIGURE 1. Color fundus photographs and autofluorescence images of 4 representative cases with a foveal-sparing phenotype of Stargardt disease (Patients 6, 11, 29, and 8), showing 4 fundus phenotypes identified in this study, respectively. Images show examples of each of 4 fundus phenotypes identified in this study: Patient 6 shows pattern 1 (patchy parafoveal atrophy surrounded by numerous yellow-white flecks); Patient 11 shows pattern 2 (numerous yellow-white flecks at the posterior pole without atrophy); Patient 29 shows pattern 3 (mottled retinal pigment epithelium changes and localized parafoveal yellow-white flecks); and Patient 8 shows pattern 4 (multiple patchy atrophic lesions, extending beyond the arcades).

−0.08 to 2.0 and −0.08 to 3.0). Two patients (4 and 26) had a logMAR visual acuity of less than 1.0 in the right eye at the most recent review, with those patients having been diagnosed with the foveal-sparing phenotype of Stargardt disease 4 years earlier, when visual acuity was 0.18 in the right eye and 0.48 in the left eye.

Color fundus photography was performed in all 40 patients. Four patterns were identified: pattern 1 (n = 22, 55%) showed patchy parafoveal atrophy surrounded by numerous yellow-white flecks; pattern 2 (n = 8, 20%) had numerous yellow-white flecks at the posterior pole without atrophy; pattern 3 (n = 7, 17.5%) had mottled

TABLE 1. Summary of Clinical Findings and Molecular Status of 40 Patients With a Foveal-Sparing Phenotypea of Stargardt Disease (*Continued*)

Patient	Onset[b] (y)	Age (y)	LogMAR Visual Acuity OD	LogMAR Visual Acuity OS	Fundus Pattern[c]	OCT CFT[d] (μm) OD	OCT CFT[d] (μm) OS	OCT ORT	ERG[e] Group	ERG[e] PERG OD	ERG[e] PERG OS	ERG[e] mfERG OD	ERG[e] mfERG OS	Mutation Status
33	39	40	0.18	0	5	126	140		NA	NA	NA	NA	NA	Not detected
34	25*	25	0.18	0	3	147	150		NA	NA	NA	NA	NA	Not detected
35	29	36	0	0.3	3	172	181		2	A	A	NA	NA	Not detected
36	40	45	0.3	0	1	NA	NA		1	A	N	NA	NA	Not detected
37	35	41	0.18	0.18	1	150	131	✓	1	ND	ND	NA	NA	Not detected
38	29*	29	−0.1	0	2	237	236		NA	NA	NA	NA	NA	Not detected
39	25	35	−0.1	0	1	237	179	✓	3	ND	ND	2	2	Not detected
40	75	75	0.18	0.18	1	194	186		NA	NA	NA	NA	NA	Not detected

A = abnormal; CFT = central foveal thickness; ERG = electroretinogram; mfERG = multifocal ERG; N = normal; NA = not available; ND = not detectable; OCT = optical coherence tomography; ORT = outer retinal tubulation; PERG = pattern ERG.

[a]The foveal-sparing phenotype was defined as foveal preservation on autofluorescence imaging, despite a retinopathy otherwise consistent with Stargardt disease.

[b]The age of onset was defined as the age at which visual loss was first noted by the patient or as the age at the latest examination for patients (labeled with*) who are not aware of any visual symptom. Two patients complained of diplopia (labeled with**).

[c]Color fundus photography identified 4 patterns: pattern 1, patchy parafoveal atrophy surrounded by numerous yellow-white flecks; pattern 2, numerous yellow-white flecks at the posterior pole without atrophy; pattern 3, mottled retinal pigment epithelial changes and/or localized parafoveal yellow-white flecks; pattern 4, multiple patchy atrophic lesions, extending beyond the arcades. One patient had a bull's-eye maculopathy appearance (Patient 33, labeled as pattern 5).

[d]The CFT was defined as the distance between inner retinal surface and inner border of retinal pigment epithelium.

[e]Patients were classified on the basis of electrophysiological findings: group 1 - normal ERGs with or without PERG P50 abnormality; group 2 - PERG P50 abnormality and additional generalized cone system abnormality; group 3 - PERG P50 abnormality and additional generalized cone and rod system abnormality. *mf*ERG findings were categorized based on the responses from central and paracentral hexagons into 2 subgroups: 1 - preserved central response surrounded by paracentral reduction; 2 - central and paracentral loss of responses.

Tartu, Estonia) in all probands.[43] The term "variants" used herein includes those sequence changes previously shown to be enriched in patients with Stargardt disease from prior studies. Null variants are those that would be expected to affect splicing, or to introduce a premature truncating codon in the protein if translated. Non-null variants (missense and in-frame deletions or insertions) were analyzed using 3 software prediction programs: SIFT (Sorting Intolerant from Tolerance; http://sift.jcvi.org/, accessed March 1, 2013),[44] PolyPhen2 (http://genetics.bwh.harvard.edu/pph/index.html, accessed March 1, 2013),[45] and the Human Splicing finder program version 2.4.1 (http://www.umd.be/HSF/, accessed March 1, 2013). Minor allele frequency for each allele was estimated with reference to the Exome Variant Server (NHLBI Exome Sequencing Project, Seattle, Washington, USA; http://snp.gs.washington.edu/EVS/, accessed March 1, 2013).

To investigate potential molecular genetic differences between patients with the foveal-sparing phenotype and those with typical disease (without foveal sparing/with foveal atrophy), the molecular data of patients with typical Stargardt disease ascertained at Moorfields Eye Hospital were reviewed. This comparison group consisted of all patients without evidence of foveal sparing on AF imaging and also harbored at least 1 *ABCA4* disease-causing variant following screening with the APEX microarray. One hundred and forty subjects from a total cohort of 438 individuals fulfilled these criteria, and the allele frequency of the most prevalent variants was compared between the group of patients with the foveal-sparing phenotype (n = 31) and the group of patients with typical Stargardt disease (n = 140).

RESULTS

THE CLINICAL FINDINGS IN THE 40 PATIENTS WITH FOVEAL-sparing Stargardt disease are summarized in Table 1. There were 22 female patients (55%) and 18 male patients (45%). The panel included 2 sibships; a sibling pair (Patients 16 and 32) and 1 set of 3 siblings (Patients 33, 34, and 35). Twenty-five patients (63%) complained of central visual loss and 2 subjects (5%) presented with diplopia, with 13 individuals (32%) having no visual symptoms. The median age of onset was 43.5 years (range, 25-75 years), and the median age at the examination was 46.5 years (range, 25-75 years). Nineteen patients (47.5%) had onset at ≥45 years of age. The mean duration of disease was 4.1 years (range, 0-25 years). The median logMAR visual acuity was 0.18 in the right eye and 0.18 in the left eye (range,

TABLE 1. Summary of Clinical Findings and Molecular Status of 40 Patients With a Foveal-Sparing Phenotype[a] of Stargardt Disease

Patient	Onset[b] (y)	Age (y)	LogMAR Visual Acuity OD	LogMAR Visual Acuity OS	Fundus Pattern[c]	OCT CFT[d] (μm) OD	OCT CFT[d] (μm) OS	OCT ORT	ERG[e] Group	ERG[e] PERG OD	ERG[e] PERG OS	ERG[e] mfERG OD	ERG[e] mfERG OS	Mutation Status
1	45	45	0	0	3	219	223		NA	NA	NA	NA	NA	[c.1411 G>A, p.Glu471Lys/c.2588 G>C, p. Gly863Ala/c.4594 G>A, p.Asp1532Asn/c.5693 G>A, p.Arg1898His]
2	33	33	0.18	0.48	1	NA	NA		3	ND	ND	NA	NA	[c.1622 T>C, p.Leu541Pro/c.3113 C>T, p.Ala1038Val/c.6089 G>A, p.Arg2030Gln]
3	53	66	0.18	0.18	1	NA	NA		2	A	A	NA	NA	[c.768 G>T, Splice site/c. 6320 G>A, p. Arg2107His]
4	37	54	1.48	0.18	1	32	39	✓	3	ND	ND	2	2	[c.1760 +1 G>T, Splice site/c.4594 G>T, p.Asg1532Tyr]
5	57	57	0.3	0.18	1	NA	NA		1	ND	ND	NA	NA	[c. 1805G>A, p. Arg602Gln/c.3898 C>T, p.Arg1300*]
6	65*	65	0.18	0	1	211	187	✓	1	N	N	NA	NA	[c.5461-10 T>C, Splice site/c. 6089 G>A, p.Arg2030Gln]
7	54*	54	0	0	1	189	198		1	A	A	NA	NA	[c. 6089 G>A, p.Arg2030Gln/c.6118 C>T, p.Arg2040*]
8	39	44	−0.1	−0.1	4	297	230	✓	3	A	A	NA	NA	[c.71 G>A, p.Arg24His/c.4577 C>T, p. Thr1526Met]
9	35*	35	0.18	0.18	2	142	154		3	ND	ND	NA	NA	[c.658 C>T, p.p.Arg220Cys/c.2588 G>C, p. Gly863Ala]
10	45	54	0.48	0.18	1	102	116		3	ND	A	NA	NA	[c.1957 C>T, p.Arg653Cys/c.5693 G>A, p.Arg1898His]
11	43	43	−0.1	0	2	170	185		1	A	A	2	2	[c.2588 G>C, p. Gly863Ala/c.4139 C>T, p.Ala1038Val]
12	36**	38	0.3	0	1	220	212	✓	1	A	A	1	1	[c.4139 C>T, p.Ala1038Val/c.4594 G>T, p.Asp1532Asn]
13	62	68	−0.1	0.48	1	196	189	✓	1	N	N	2	2	[c.4222 T>C, p.Trp1408Arg/c.4918 C>T, p.Arg1640Trp]
14	36	44	0.48	0.48	3	79	89		1	A	A	NA	NA	[c.4222 T>C, p.Trp1408Arg/c.4918 C>T, p.Arg1640Trp]
15	46*	46	−0.1	−0.1	3	NA	NA		1	A	A	NA	NA	[c.4469 G>A, p.Cys1490Tyr/c. 6089 G>A, p.Arg2030Gln]
16	44*	44	0.18	0	2	NA	NA		1	A	A	NA	NA	[c.6079 C>T, p.Leu2027Phe/c.6079 C>T, p.Leu2027Phe]
17	48	73	0.18	3	4	135	86	✓	2	A	ND	NA	NA	[c.4956 T>G, p.Tyr1652*]
18	56	57	0	0	2	254	273		1	ND	A	NA	NA	[c.5018+2 T>C, Splice site]
19	53*	53	0.48	0.18	1	137	133		1	A	A	NA	NA	[c.5461-10 T>C, Splice site]
20	49	58	0.18	0	1	256	222	✓	1	A	N	1	1	[c.5461-10 T>C, Splice site]
21	47**	47	0.3	0.3	1	239	202	✓	1	A	A	1	1	[c.1805 G>A, p.Arg602Gln]
22	50*	50	0.48	0.18	1	263	261	✓	1	N	N	NA	NA	[c.1957 C>T, p.Arg653Cys]
23	39*	39	0	−0.1	2	225	228		1	N	N	NA	NA	[c.2588 G>C, p. Gly863Ala]
24	55	57	0.48	0.48	1	117	74		1	ND	ND	NA	NA	[c.3602 T>G, p.Leu1201Arg]
25	50	54	0.48	0.18	1	147	144	✓	3	ND	ND	NA	NA	[c.3602 T>G, p.Leu1201Arg]
26	43	47	2	0.18	1	70	52		1	ND	ND	NA	NA	[c.4319 T>C, p.Phe1440Ser]
27	30	51	0.3	0.3	1	75	79	✓	3	A	A	NA	NA	[c.4685 T>C, p.Ile1562Thr]
28	29	34	0.18	0.18	3	132	107		1	A	A	NA	NA	[c.4926 C>G, p.Ser1642Arg]
29	52*	52	0.18	0.18	3	180	200		1	ND	ND	2	2	[c.5882 G>A, p.Gly1961Glu]
30	28	28	−0.1	−0.1	2	NA	NA		1	N	ND	NA	NA	[c.6079 C>T, p.Leu2027Phe]
31	40*	40	−0.1	−0.1	2	222	223	✓	NA	NA	NA	NA	NA	[c.6079 C>T, p.Leu2027Phe]
32	45	48	0.18	3	1	237	252	✓	NA	NA	NA	NA	NA	NA

Continued on next page

central retinal atrophy.[13,15] Foveal-sparing forms of Stargardt disease may thus reflect a distinct pathogenesis.

The present study describes the clinical findings and molecular genetic characteristics of "foveal-sparing" Stargardt disease in a large cohort from a single center. The molecular data of the cohort with the foveal-sparing phenotype are compared with *ABCA4* variants observed in patients with Stargardt disease but without foveal sparing.

METHODS

• PATIENTS: AF images of the right eyes of 438 individuals with a clinical diagnosis of retinopathy compatible with Stargardt disease were surveyed and 40 patients were identified with an apparently normal AF signal at the fovea (foveal sparing). After informed consent, blood samples were collected and genomic DNA was extracted from the peripheral blood leukocytes. The protocol of the study adhered to the provisions of the Declaration of Helsinki and was approved by the local Ethics Committee of Moorfields Eye Hospital.

For the purposes of this report, patients presenting to the hospital with signs of atrophy within the macula, bilaterally, with or without surrounding flecks were potentially included as having Stargardt disease. Patients with a stationary visual dysfunction were excluded. A careful drug history was taken to allow exclusion of those with retinotoxic maculopathy. Patients with a dominant family history were excluded. Where a family history was not extensive, or whenever 2 generations were affected, the *RDS/PRPH2* gene, with its coding region and intron-exon boundaries, was sequenced. In those patients over 50 years of age, care was taken not to include cases of atrophic age-related macular degeneration in which there were soft drusen, or patients with maternally inherited diabetes and deafness in whom the distribution of atrophy and autofluorescence appearance had a distinctive appearance. The m.3243A>G variant was assayed if this phenotype was in any way suggested.

• CLINICAL ASSESSMENT: A detailed medical history was obtained and a comprehensive ophthalmologic examination was performed for all 40 patients. The age of onset was defined as the age at which visual loss was first noted by the patient or as the age at the latest examination for asymptomatic patients. The duration of the disease was calculated as the difference between age at onset and age at the latest examination. Assessment included best-corrected visual acuity, dilated ophthalmoscopy, color fundus photography, AF imaging, SDOCT imaging, and electrophysiological assessment. Best-corrected Snellen visual acuity was converted to equivalent logMAR visual acuity.

Color fundus photography was performed with a TRC-501A retinal fundus camera (Topcon, Tokyo, Japan). AF images before 2009 were obtained with an HRA 2 (Heidelberg Engineering, Heidelberg, Germany; excitation light 488 nm; barrier filter 500 nm; field of view 30 × 30 degrees),[34] and images after 2009 were undertaken using the Spectralis with viewing module version 5.1.2.0 (Heidelberg Engineering; excitation light 488 nm; barrier filter 500 nm; fields of view 30 × 30 degrees and 55 × 55 degrees).[35]

SDOCT was undertaken with the Spectralis with viewing module version 5.1.2.0. The SDOCT protocol included a horizontal linear scan (100 B-scans averaged to improve the signal-to-noise ratio) centered on the fovea, where possible, and a volume scan (minimum of 19 B-scan slices, 20 × 20 degrees). The HEYEX software interface (version 1.6.2.0; Heidelberg Engineering) was used for retinal thickness measurement.[36] Central foveal thickness was defined as the distance between the inner retinal surface and the inner border of the RPE.[36,37] Evidence of outer retinal tubulation was assessed from all the B-scan slices of each eye by 2 authors (K.F. and A.R.W.).[35,38]

• ELECTROPHYSIOLOGY: Electrophysiological assessment included full-field electroretinogram (ERG) and pattern electroretinogram (PERG) recorded with gold foil electrodes that incorporated the standards of the International Society for Clinical Electrophysiology of Vision.[39–41] The full-field ERGs were used to assess generalized rod and cone system function and included: (1) dark-adapted dim flash 0.01 candela-seconds per square meter ($cd \cdot s \cdot m^{-2}$); (2) dark-adapted bright flash 11.0 $cd \cdot s \cdot m^{-2}$; (3) light-adapted 3.0 $cd \cdot s \cdot m^{-2}$ 30 Hz flicker; and (4) light-adapted 3.0 $cd \cdot s \cdot m^{-2}$ at 2 Hz. The PERG P50 component and multifocal electroretinogram (mfERG) were used to assess macular function. Some patients had mfERG recording (RETIscan System; Roland Consult, Wiesbaden, Germany) with a stimulus consisting of 61 scaled hexagons covering in total a visual field of 55 degrees, at a viewing distance of 33 cm.[42] All main components of the ERG and the PERG P50 component were used to classify patients into 3 groups; this is a partial modification of a previous report[9]: (1) patients with normal ERGs with or without a PERG P50 abnormality; (2) subjects with a PERG P50 abnormality and additional generalized cone-mediated ERG abnormality (assessed with photopic ERGs); and (3) individuals with a PERG P50 abnormality and generalized cone system electrophysiological abnormality and additional generalized rod-mediated ERG abnormality (assessed using scotopic ERGs).

• MUTATION SCREENING AND MOLECULAR GENETIC ANALYSIS: Blood samples were collected in EDTA tubes and DNA was extracted with a Nucleon Genomic DNA extraction kit (BACC2; Tepnel Life Sciences, Manchester, United Kingdom), or the Qiagen Gentra Puregene blood kit (Qiagen, Venlo, Netherlands). Mutation screening of *ABCA4* was performed with the arrayed primer extension (APEX) microarray (ABCR400 chip, Asper Ophthalmics,

Clinical and Molecular Analysis of Stargardt Disease With Preserved Foveal Structure and Function

KAORU FUJINAMI, PANAGIOTIS I. SERGOUNIOTIS, ALICE E. DAVIDSON, GENEVIEVE WRIGHT, RAVINDER K. CHANA, KAZUSHIGE TSUNODA, KAZUO TSUBOTA, CATHERINE A. EGAN, ANTHONY G. ROBSON, ANTHONY T. MOORE, GRAHAM E. HOLDER, MICHEL MICHAELIDES, AND ANDREW R. WEBSTER

• PURPOSE: To describe a cohort of patients with Stargardt disease who show a foveal-sparing phenotype.
• DESIGN: Retrospective case series.
• METHODS: The foveal-sparing phenotype was defined as foveal preservation on autofluorescence imaging, despite a retinopathy otherwise consistent with Stargardt disease. Forty such individuals were ascertained and a full ophthalmic examination was undertaken. Following mutation screening of *ABCA4*, the molecular findings were compared with those of patients with Stargardt disease but no foveal sparing.
• RESULTS: The median age of onset and age at examination of 40 patients with the foveal-sparing phenotype were 43.5 and 46.5 years. The median logMAR visual acuity was 0.18. Twenty-two patients (22/40, 55%) had patchy parafoveal atrophy and flecks; 8 (20%) had numerous flecks at the posterior pole without atrophy; 7 (17.5%) had mottled retinal pigment epithelial changes; 2 (5%) had multiple atrophic lesions, extending beyond the arcades; and 1 (2.5%) had a bull's-eye appearance. The median central foveal thickness assessed with spectral-domain optical coherence tomographic images was 183.0 μm (n = 33), with outer retinal tubulation observed in 15 (45%). Twenty-two of 33 subjects (67%) had electrophysiological evidence of macular dysfunction without generalized retinal dysfunction. Disease-causing variants were found in 31 patients (31/40, 78%). There was a higher prevalence of the variant p.Arg2030Gln in the cohort with foveal sparing compared to the group with foveal atrophy (6.45% vs 1.07%).
• CONCLUSIONS: The distinct clinical and molecular characteristics of patients with the foveal-sparing phenotype are described. The presence of 2 distinct phenotypes of Stargardt disease (foveal sparing and foveal atrophy) suggests that there may be more than 1 disease mechanism in *ABCA4* retinopathy. (Am J Ophthalmol 2013;156: 487–501. © 2013 by Elsevier Inc. All rights reserved.)

STARGARDT DISEASE IS AN AUTOSOMAL RECESSIVE disorder caused by mutations in the *ABCA4* gene.[1,2] It is the most common single-gene retinal degeneration, with a reported prevalence of 1:10 000.[3,4] Most cases typically present with central visual loss within the first 2 decades of life, and during the course of the disorder there is macular atrophy with yellow-white flecks in the posterior pole, at the level of the retinal pigment epithelium (RPE).[4,5] However, Stargardt disease is associated with a variable phenotype and severity.[4–13] Autofluorescence (AF) imaging and electroretinography may assist the diagnosis, and parameters such as age of onset, visual acuity, AF pattern, and the nature of the electrophysiological findings assist both in the determination of disease severity and in the provision of prognostic information.[5,8,9,11,14] Increasingly, high-resolution imaging using spectral-domain optical coherence tomography (SDOCT) is providing insights into the retinal architectural changes that occur in Stargardt disease.[12,14–19]

There is wide phenotypic variability in *ABCA4* retinopathy[3,4,6,8,10,12,20–24] and sequence variants in *ABCA4* have also been implicated in cone dystrophy, cone-rod dystrophy, and "retinitis pigmentosa" in addition to Stargardt disease.[2,21,25–28] There is also extensive allelic heterogeneity, with more than 700 sequences in the *ABCA4* gene having been reported to date.[2,3,6,8,10,12,20–22,25–27,29,30-33] The phenotypic variability and the high genetic heterogeneity have confounded attempts to examine genotype-phenotype correlations comprehensively.[4,31,32]

A cohort of Stargardt disease patients who had better visual acuity than "typical" Stargardt disease patients, and who showed sparing of the fovea on funduscopy, has been described.[5] There are also reports of patients with "late-onset" Stargardt disease, including individuals with a foveal-sparing phenotype, who harbor *ABCA4* variants.[6,12,22] In those reports, SDOCT images demonstrated a well-preserved foveal structure including the neurosensory retina,[6,12,22] which differed from previous observations of early foveal photoreceptor damage in "typical" Stargardt disease with

Accepted for publication May 6, 2013.
From University College London, Institute of Ophthalmology, London, United Kingdom (K.F., P.I.S., A.E.D., G.W., R.K.C., C.A.E., A.G.R., A.T.M., G.E.H., M.M., A.R.W.); Moorfields Eye Hospital, London, United Kingdom (K.F., P.I.S., A.E.D., G.W., R.K.C., C.A.E., A.G.R., A.T.M., G.E.H., M.M., A.R.W.); Laboratory of Visual Physiology, National Institute of Sensory Organs, National Tokyo Medical Center, Tokyo, Japan (K.F., K.Tsunoda); and Department of Ophthalmology, Keio University, School of Medicine, Tokyo, Japan (K.F., K.Tsubota).
Inquiries to Professor Andrew R. Webster, University College London, Institute of Ophthalmology, 11-43 Bath Street, London EC1V 9EL, United Kingdom; e-mail: andrew.webster@ucl.ac.uk

0002-9394/$36.00
http://dx.doi.org/10.1016/j.ajo.2013.05.003